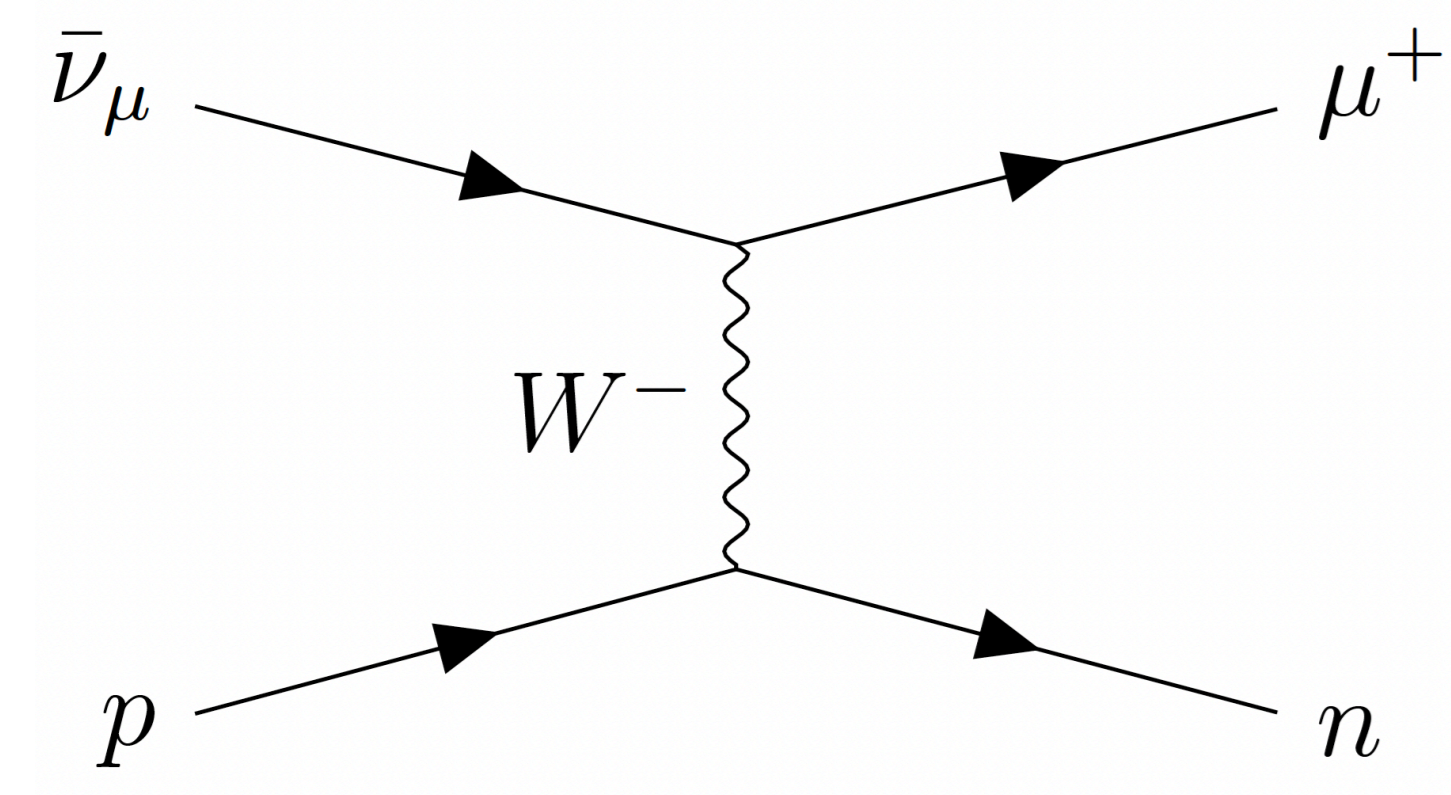


1. $\bar{\nu}_\mu$ -Hydrogen Charged-Current Elastic Interactions

(Anti)neutrino-Hydrogen Interactions are free of nuclear effects. The CCE ($\bar{\nu}_\mu H \rightarrow \mu^+ n$) interactions can be used to determine the axial-vector form factor and radius of the proton and the absolute $\bar{\nu}_\mu$ flux.

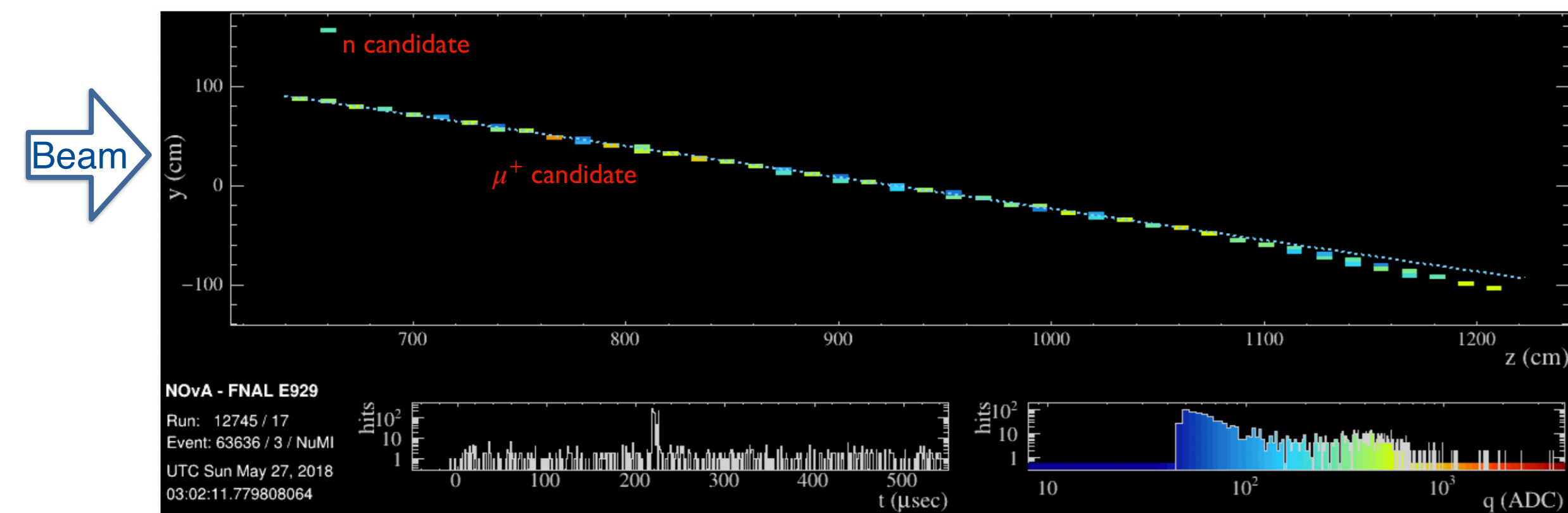


Feynman diagram for $\bar{\nu}_\mu H \rightarrow \mu^+ n$

$$\frac{d\sigma}{dQ^2}(E_\nu, Q^2) = \frac{G_F^2 |V_{ud}|^2 M^2}{2\pi E_\nu^2} \left[(\tau + r_\ell^2) A(\nu, Q^2) + \frac{\nu}{M^2} B(\nu, Q^2) + \frac{\nu^2}{M^4} \frac{C(\nu, Q^2)}{1 + \tau} \right]$$

The structure functions A, B, and C encode the nucleon vector form factors (F_1^V, F_2^V) and the axial form factor $F_A(Q^2)$.

2. The NOvA Near Detector



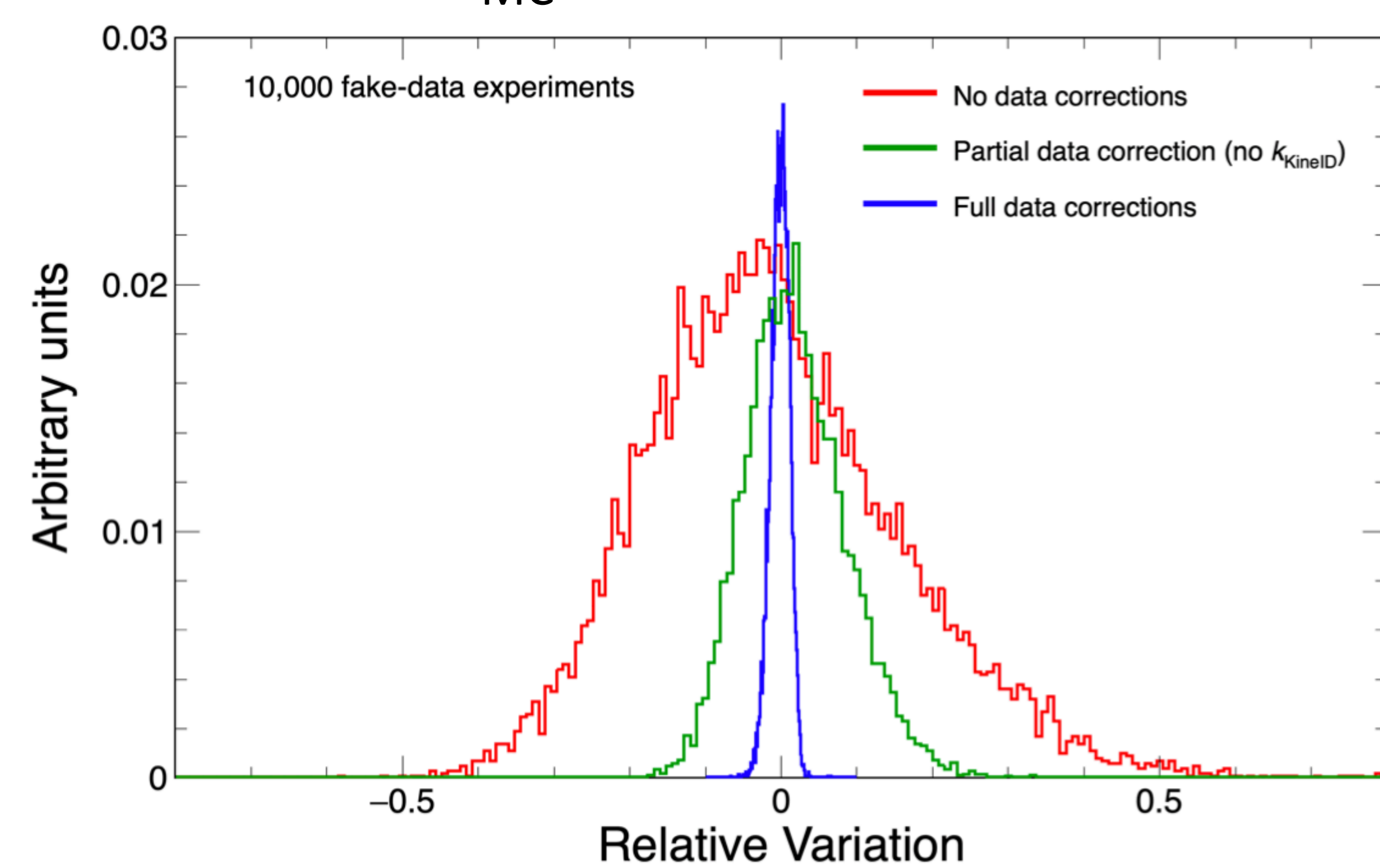
Display of a CCE like event from NOvA data

- Antineutrino NuMI beam: 93% $\bar{\nu}_\mu$, $\langle E \rangle \sim 1.9$ GeV, 1.2×10^{21} POT.
- Near Detector (ND): Liquid scintillator (CH_2) inside PVC cells containing 10.8% hydrogen by mass.
- CCE signature : Long reconstructed track associated with isolated object originating from neutron interaction.

4. Data Corrections

- Signal Region (SR): selected events.
- Control Regions (CR): Data-driven background constraints obviating the limitations of the Monte Carlo (MC) simulations.
- Data corrections derived from the CRs :

$$\epsilon_{\text{Bkg}} = \epsilon_{\text{MC}} \times \frac{\epsilon_{\text{Data}}^{\text{CR}}}{\epsilon_{\text{MC}}^{\text{CR}}} = \epsilon_{\text{MC}} \times k_{\text{cut}}$$



Variation of background in SR pre and post data corrections

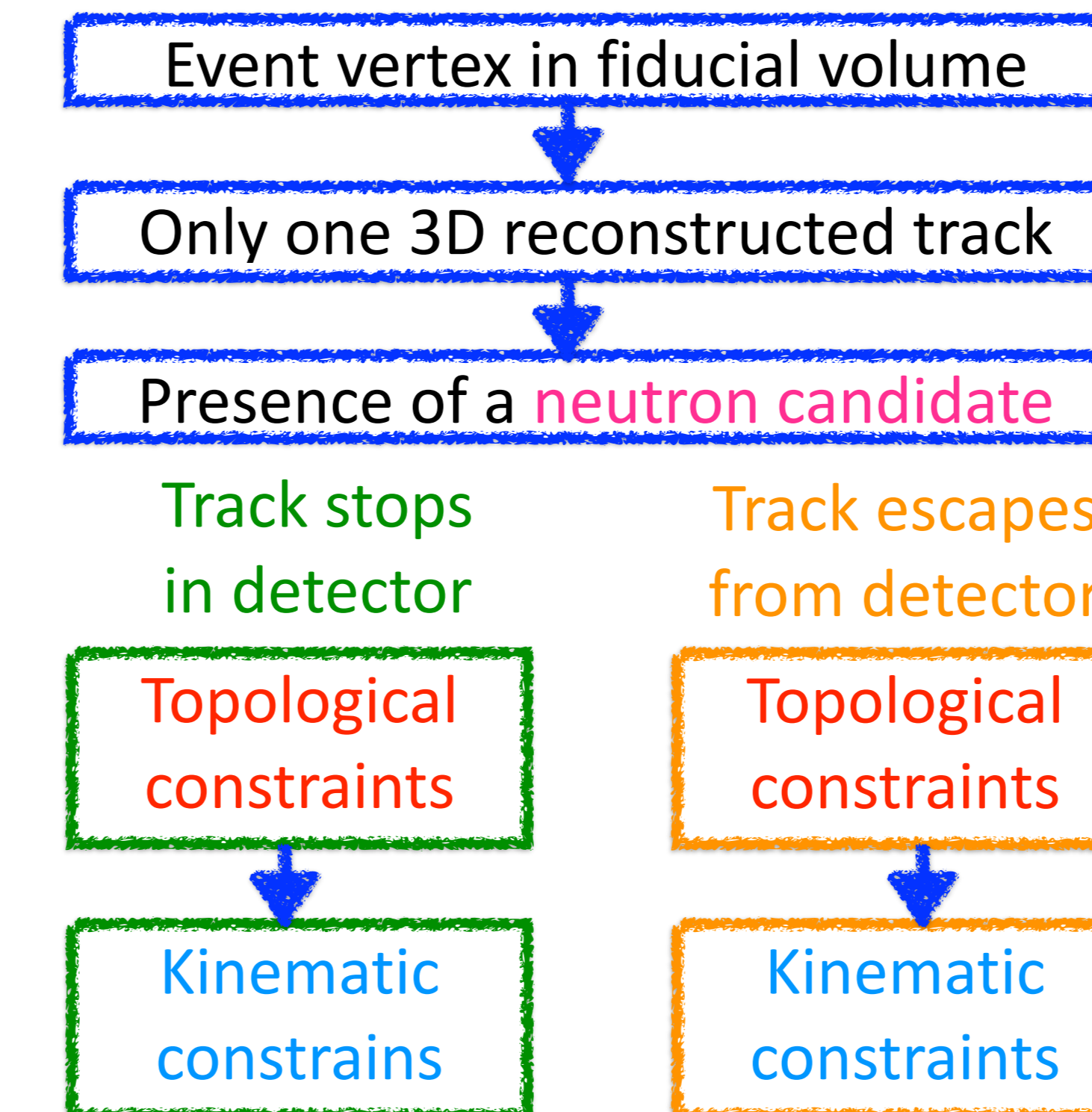
5. Systematic Uncertainties

- Repeat complete analysis after shifting each parameter.
- Three Data Correction Factors : k_{nc} , k_{HitID} and k_{KineID} .
- The correction factors are re-evaluated for each variation.
- Systematic uncertainties obtained from comparing the shifted results from the nominal.

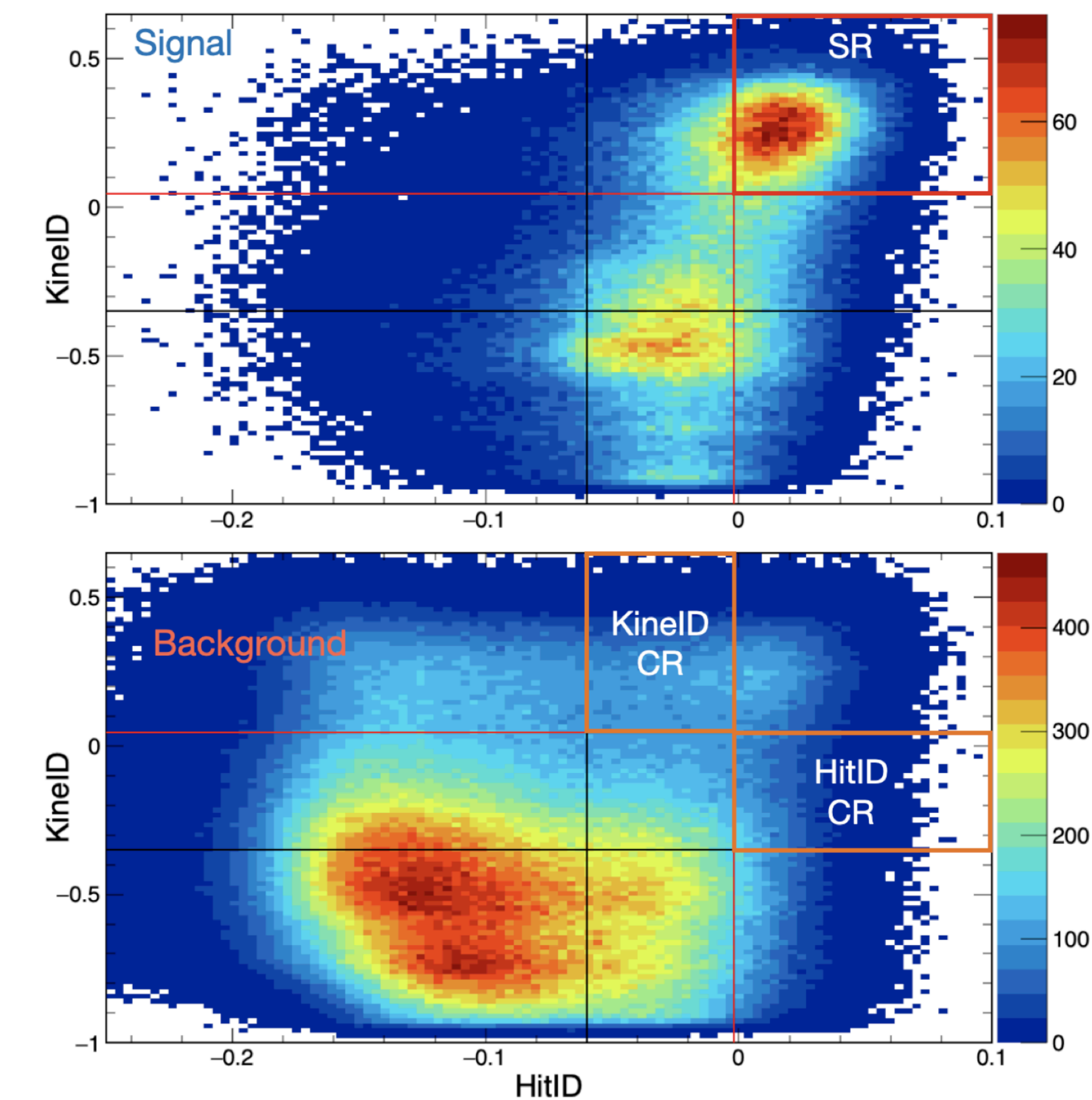
Source	Contained (%)	Uncontained (%)	Correlation
Normalization	0.9	0.9	1.00
Background estimate	1.2	1.3	0.96
QE modelling	0.8	1.3	0.30
Neutron detection	1.1	1.1	-0.47
Muon energy scale	0.6	0.2	-0.07
Muon angle scale	0.6	0.2	-0.23
Detector	1.0	0.5	-0.58
Systematics (w/o flux)	2.4	2.4	

- All systematic uncertainties related to detector and reconstruction effects are anti-correlated for the two samples.

3. Selection of $\bar{\nu}_\mu H \rightarrow \mu^+ n$ events



- **Neutron Candidate**: Closest isolated object to the calculated neutron line of flight.
- **HitID**: Topological constraint based on the location and energy of hits/tracks (14 input variables).
- **KineID**: Global event kinematics to select H at rest (7 input variables).

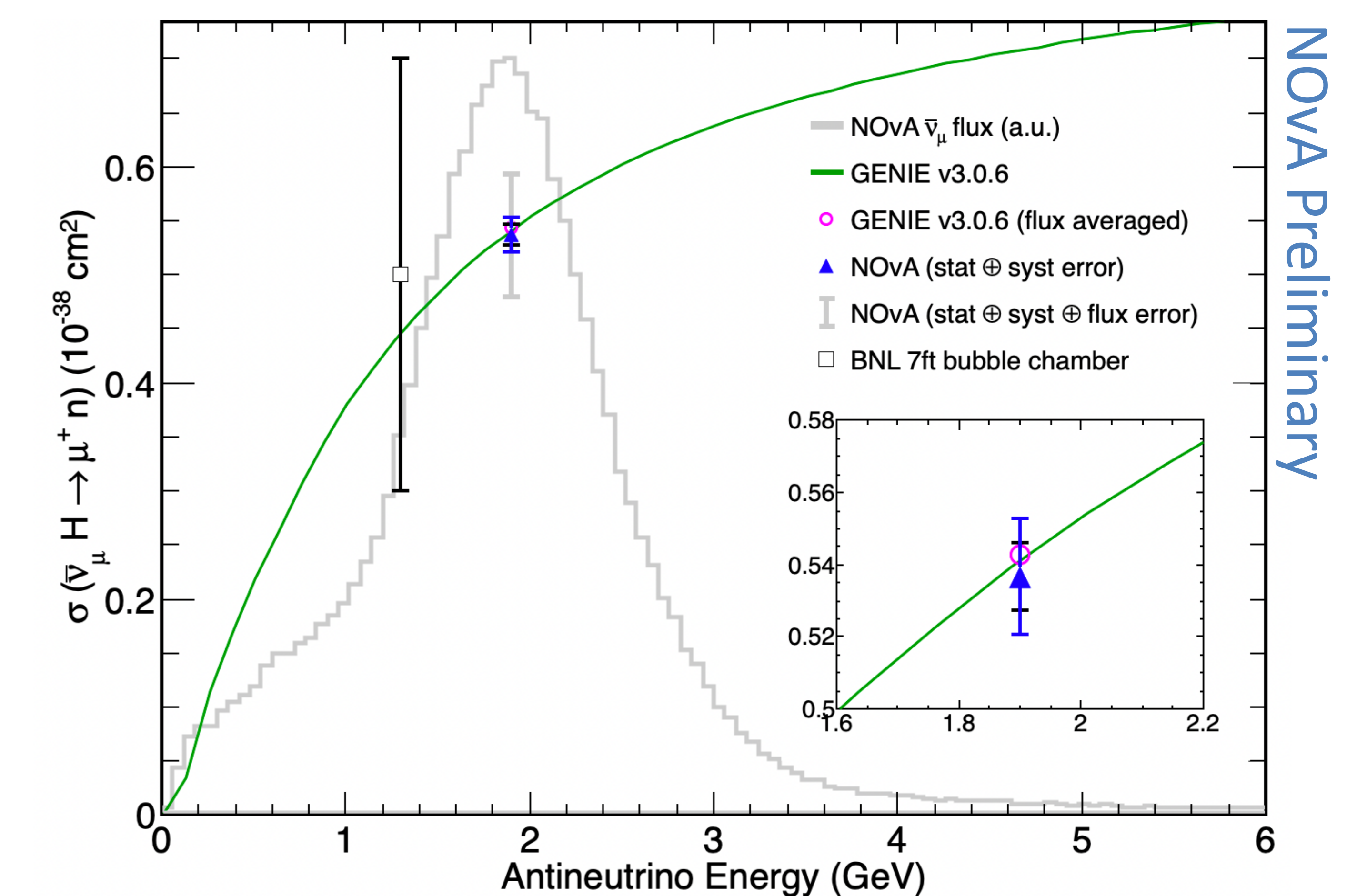


Definition of SR and CR in HitID-KineID plane

6. Results for Total Cross Section

	Signal	Background	Total	Data	Data/Expected
Contained	15,103	27,839	42,941	43,644	$0.985 \pm 0.008 \pm 0.013$
Uncontained	20,670	43,544	64,214	63,248	$1.016 \pm 0.010 \pm 0.013$

- Total signal — Observed : $35,509 \pm 679(\text{stat})$, Expected : $35,773$
Largest (anti)neutrino-hydrogen sample measured to date.



- $\sigma_{\text{CCE}} = 0.538 \pm 0.009(\text{stat}) \pm 0.010(\text{syst}) \pm 0.055(\text{flux}) \times 10^{-38} \text{ cm}^2$
Most precise CCE cross section to date.

[1] S. Abubakar et al. (NOvA), Phys. Rev. Lett. **136**, 011802 (2026), arXiv:2509.04361 [hep-ex].

[2] S. Abubakar et al. (NOvA Collaboration), to appear on arXiv [hep-ex]

[3] H. Duyang, B. Guo, S. R. Mishra, and R. Petti, Phys Lett. B **795**, 424 (2019), arXiv:1902.09480 [hep-ph].

[4] R. Petti, Phys. Lett. B **834**, 137469 (2022), arXiv:2205.10396 [hep-ph]

[5] R. Petti, R. J. Hill, and O. Tomalak, Phys. Rev. D **109**, L051301 (2024), arXiv:2309.02509 [hep-ph].

[6] H. Duyang, B. Guo, S. R. Mishra, and R. Petti, Eur. Phys. J. Plus **139**, 1014 (2024), arXiv:1809.08752 [hep-ph]